Chapter 4.

THE ENERGY ANALYSIS OF FIELD-EVAPORATED IONS.

4.1 Experimental Considerations.

It is known that if a mass-spectrometer is used to analyse the field-evaporation products from a refractory metal specimen in poor vacuum the products are found to include many ions which are attributable to the interaction of nitrogen, oxygen and water vapour with the specimen. This is the case when the evaporation is occurring at a relatively low rate (a few planes per second) or under pulsed evaporation conditions where there is sufficient time between pulses for contaminants to build up on the surface. At very high evaporation rates which are sustained for the time necessary for many planes to evaporate, it is likely that only the first plane to be evaporated will be severely affected by corrosion processes: the supply of contaminants will be inhibited at the evaporation field of a refractory metal by the need for the contaminants to penetrate the high-field barrier without being ionized. This field-ionized current of contaminants may be seen with an energy analyser as a low-energy signal: the contaminants have low ionization potentials compared to helium, and at helium BIV or higher fields they will mostly be ionized far from the surface, if coming from the gas phase. This low-energy signal may be used to determine whether or not the metal-ions evaporated under a particular set of conditions are likely to have been affected by corrosion processes. Provided that the number of evaporated metal ions detected greatly exceeds the number of contaminant ions caught in the same period of time, pure field-evaporation

rather than corrosion is likely to be the dominant process. This is not necessarily the case for non-refractory metals; experiments in field desorption, to be described below, show that under some conditions the field-evaporation behaviour of copper and silver may be dominated by a thin film of contaminant, which is resistant to field-evaporation and field-ionization.

In view of the relatively poor vacuum of the prototype energy analyser it was clear that any attempt to superpose the metal ion spectra obtained by evaporating the specimen with a series of nanosecond pulses over a period of seconds would lead to misleading results, if each pulse only removed a fraction of a monolayer of the specimen surface. To obtain sensible metal ion spectra using pulsed evaporation it would be necessary ro remove a minimum of 2 planes per pulse, in the hope that any field-adsorbed impurities would evaporate with the first plane to be evaporated. This process leads to unacceptably high evaporation rates, using nanosecond pulses: to obtain the required rate ($\sim 10^9$ planes/second, sustained while 2 or more planes evaporate) the vacuum evaporation field has to be raised to a value at which premature mechanical failure of the specimen becomes a virtual certainty.

There is a much higher chance of success if the evaporation pulse is some tens of microseconds long, rather than a few nanoseconds. The evaporation rate is now of the order of 10^5 planes/second; the contamination is still 10^5 less than would be the case if the rate was 1 plane/second (either continuous evaporation or repetitive pulsed evaporation). Against this must be set the fact that the energy loss processes due to pulse effects will be different to those found under nanosecond-pulsed conditions, so that direct comparison between the energy spectra and atom-probe spectra is not

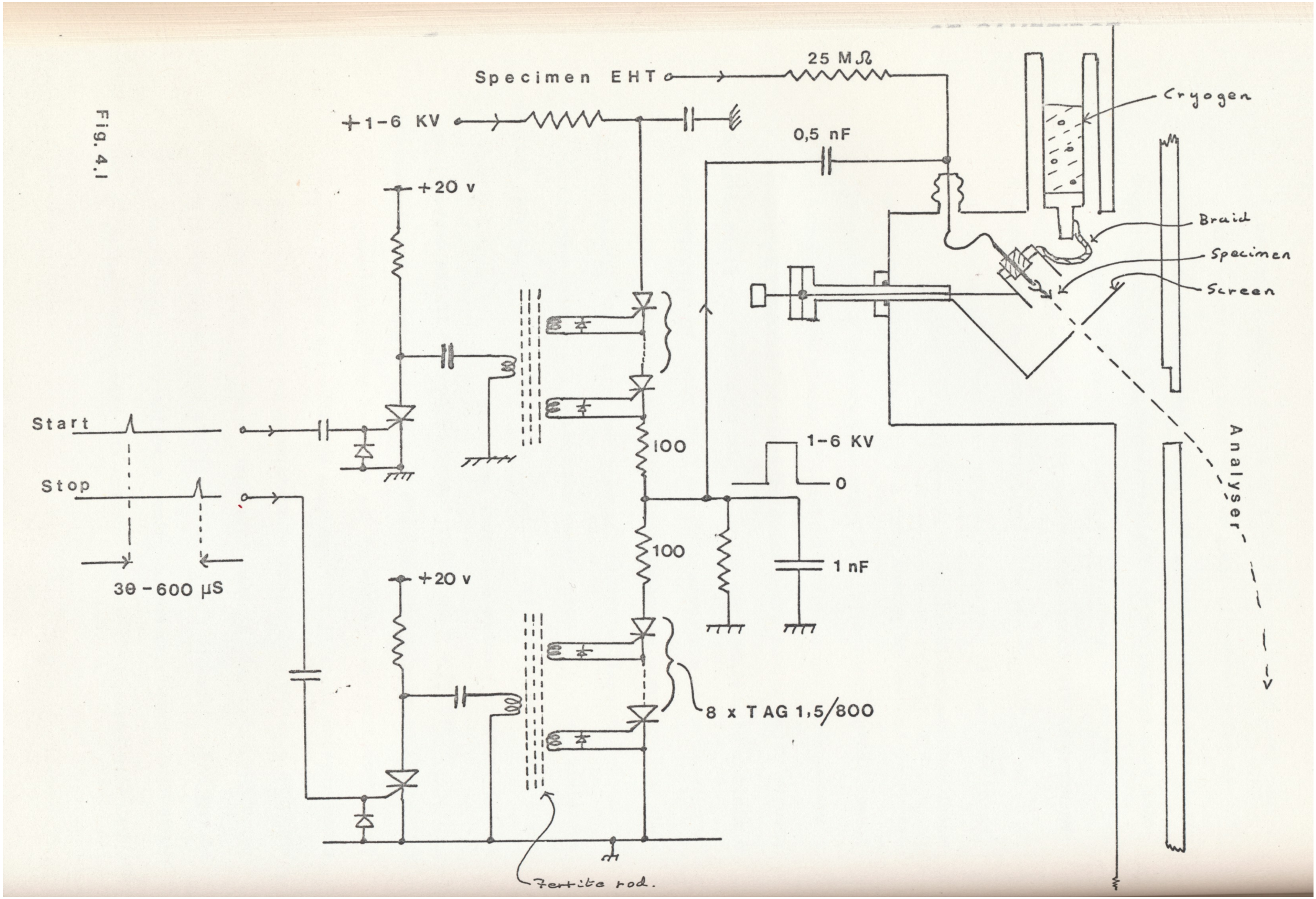
Specimen EHT
25 MΩ
+1-6 KV
0,5 nF
Cryogen
Braid
Specimen
Screen
+20 v
Start
Stop
100
1-6 KV
0
100
1 nF
30 - 600 µS
+20 v
8 x TAG 1,5/800
Analyser
Ferrite rod.

Fig. 4.1

possible. There will still be pulse-effects: there is a high probability that some ions will be evaporated during the relatively slow rising edge of such an evaporation pulse. Provided that the flat top of the evaporation pulse is maintained until the evaporation rate has been reduced substantially by the blunting of the specimen, very few of the ions will have been affected by the falling edge of the pulse, which will proabably fall over a time long compared to the time taken for the ions to leave the specimen field. Any energy losses which are intrinsic to the field-evaporation process (plasmon losses, etc.) are expected to be insensitive to the evaporation rate, and they will therefore be similar for the nanosecond and microsecond-pulse evaporation spectra.

4.2 Experimental Technique.

An electronic pulser capable of delivering positive pulses with lengths between 30 μS and 1mS, with risetime and falltime less than 300 nS, and pulse-height between 50 volts and 6 kV, was constructed. This pulser uses two high-voltage thyristor stacks as switches. One switch briefly connects a small storage capacitor to a high voltage supply to commence the output pulse; the storage capacitor maintains the output voltage during the output pulse; the second switch then terminates the pulse by discharging the capacitor. The microsecond pulse was coupled to the specimen by a coupling capacitor (fig(4.1)) in the standard atom-probe arrangement; the pulse line is now not terminated by a 50Ω resistor. The use of a terminated pulse line would preclude the use of this type of pulser and would require an unnecessarily high-powered pulse-generating circuit.

The mode of operation of the energy analyser to detect field-evaporated ions was as follows. The specimen was manipulated until a suitable part of the image was over the probe-hole. The specimen and screen positions were then adjusted until the image-gas spectrum was properly focussed on the detector. The specimen voltage was then adjusted until slight evaporation took place when a pulse was applied. The pulser voltage was typically 1500 volts for 10 KV specimen voltage. The image gas was then removed and a large increment of voltage was added to the specimen voltage (typically an extra 450 volts). The energy-analyser field was then adjusted so that ions with a maximum energy $ne(V_{tip} + V_{pulse})$ would be detected at the high-energy end of the detector. The pulser was then fired, using the 'X' electronic flash contacts on the camera to trigger the pulse, using a shutter speed of 1/60 second to minimize the background channel-plate noise on the spectrum. If any significant number of metal ions were seen to arrive at the detector, further spectra were recorded until the evaporation rate was low again. The specimen and analyser voltages were then raised again, and a further sequence of spectra recorded, without readmitting any helium to the system. When sufficient spectra had been recorded the image gas was readmitted to the system, so that the state of the field-ion image and the focus of the energy analyser could be checked.

The background noise level using this technique was very low. The number of apparent ions detected when the camera shutter was operated with the pulser disconnected, or at too low a voltage for evaporation to occur, was of the order of 5, over the whole detector area. When evaporated ion spectra were being recorded the film was generally overdeveloped to ensure maximum contrast and

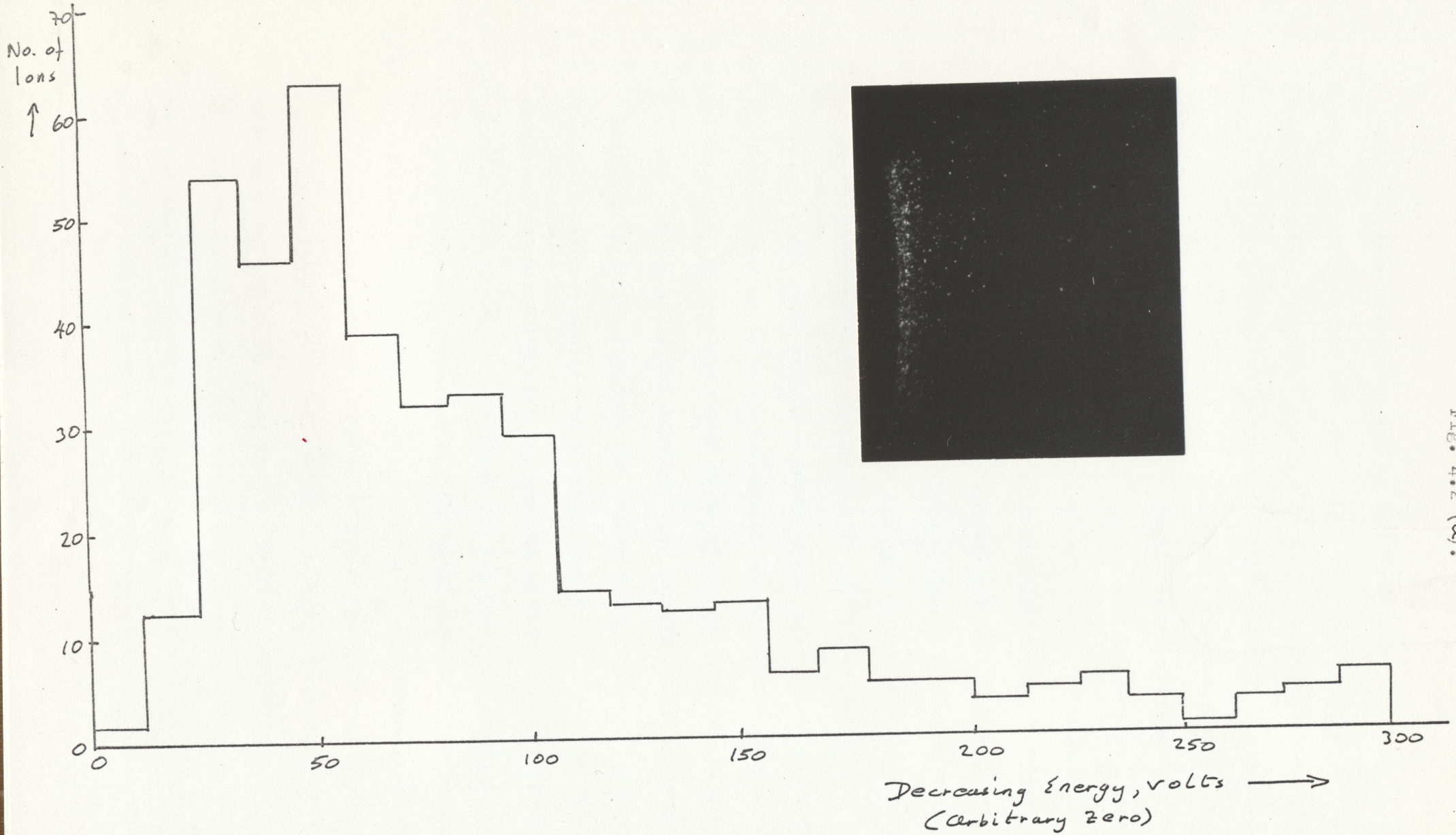
No. of Ions
70
60
50
40
30
20
10
0
0
50
100
150
200
250
300
Decreasing Energy, volts
(Arbitrary Zero)

Fig. 4.2 (a).

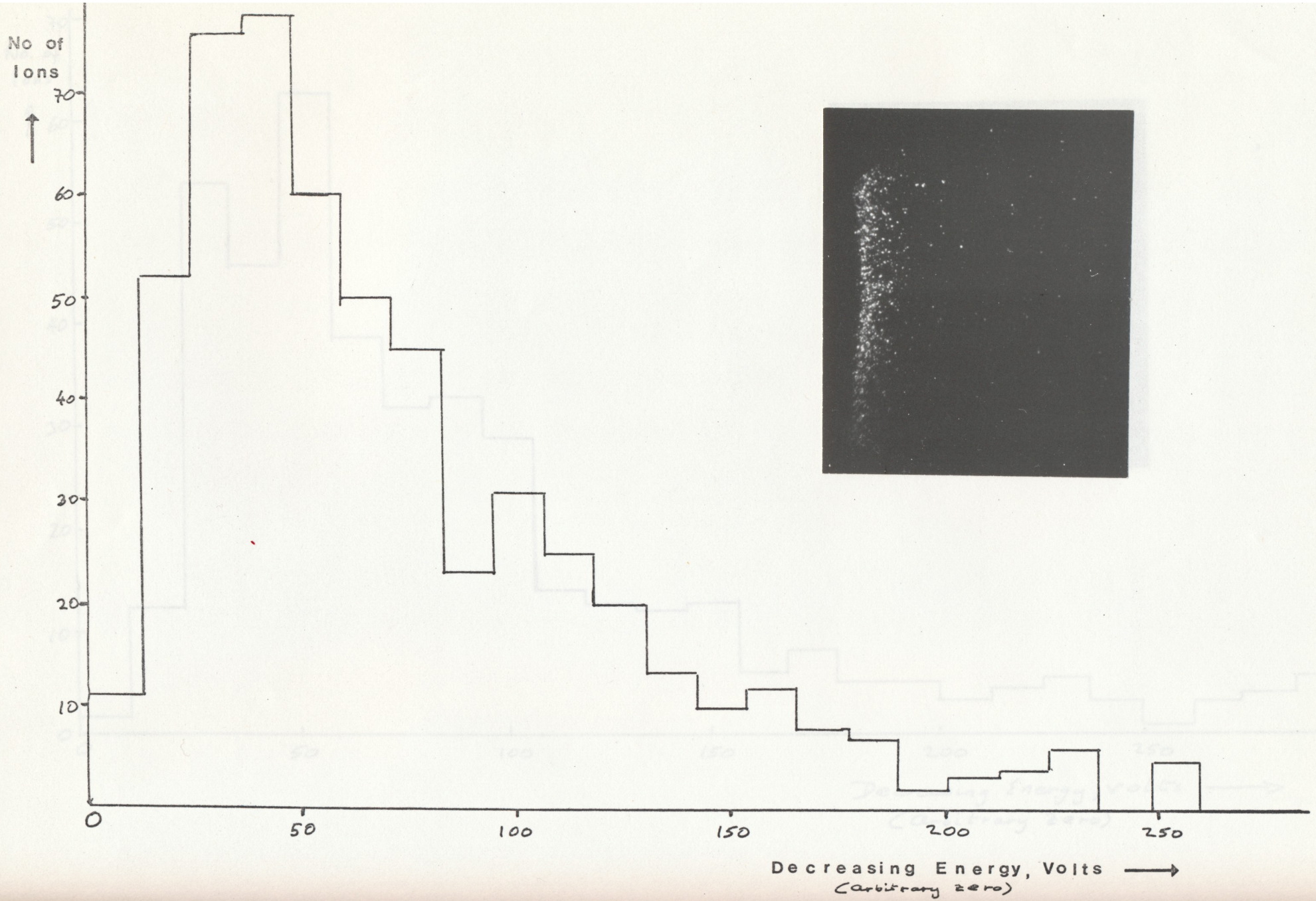
No of Ions
70
60
50
40
30
20
10
0
50
100
150
200
250
Decreasing Energy, Volts
(arbitrary zero)

Fig. 4.2 (b).

Fig. 4.3

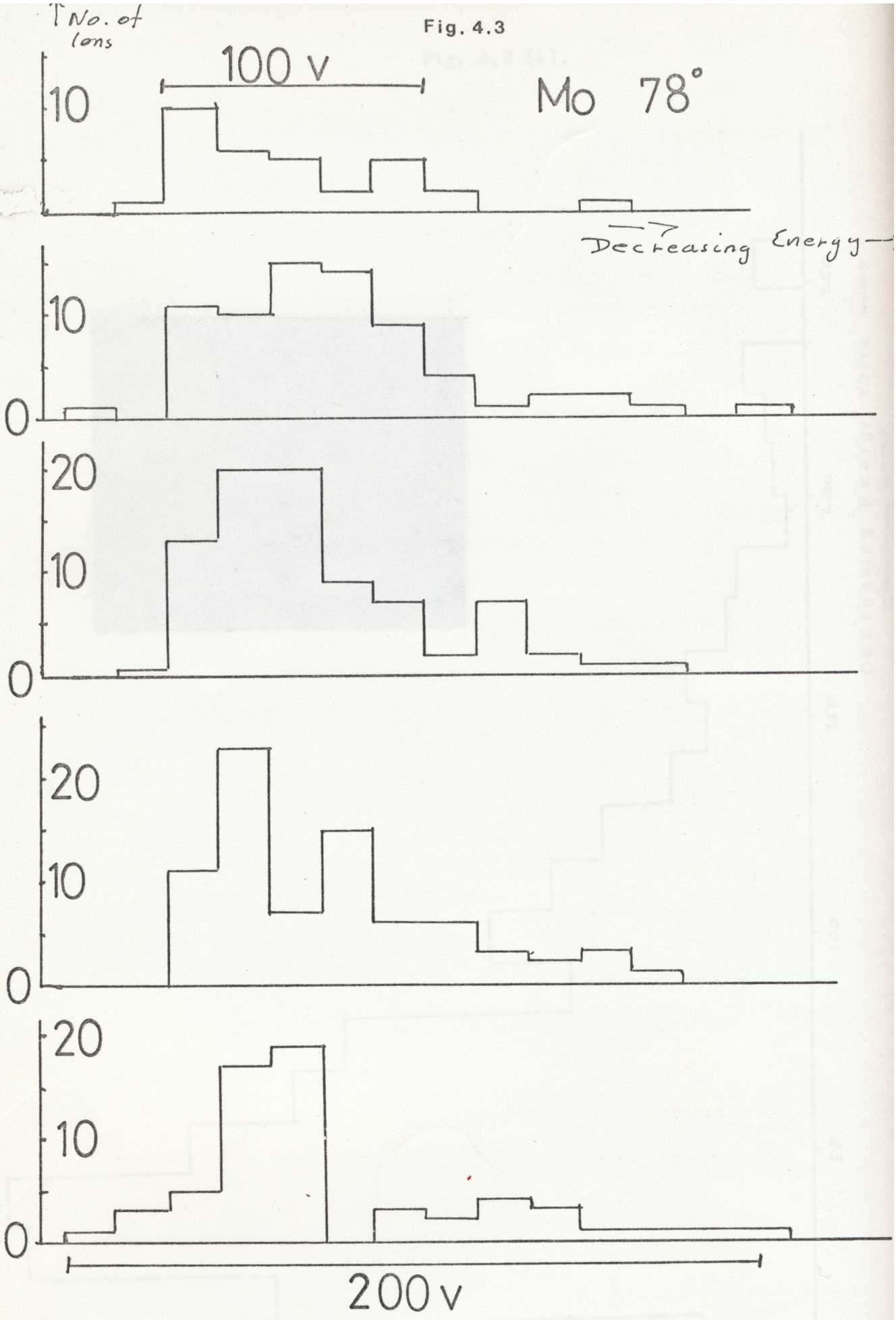
No. of Ions
100 v
Mo 78°
10
Decreasing Energy
10
0
20
10
0
20
10
0
20
10
0
200 v

the maximum chance of detecting weakly-recorded ions. The development time was generally 15 minutes in 1:1 D 76 for Tri-X film.

Some typical spectra are shown in fig(4.2). The scintillations due to the arrival of individual ions are clearly seen. The photographs of spectra were converted to histograms showing the total number of ions with an energy in a particular range. A graticule of equispaced lines, with a radius of curvature the same as that of a photograph of a helium spectrum, was ruled on a celluloid film which was laid over a 10" x 8" print of the metal spectrum; the number of ions recorded between adjacent lines was then counted 'by hand' to obtain the histogram. The energy scale of the histogram was obtained from the movement of a helium peak when a known voltage was added to the specimen voltage. The results of this procedure for various molybdenum specimens are shown in fig(4.2) and fig(4.3), for large and small evaporations per pulse respectively.

Two features of these spectra are noteworthy. Firstly, the ions are found to have a very large energy spread, comparable to that found in the atom-probe. In the atom-probe many evaporation pulses are needed at a particular standing voltage and pulse voltage before the evaporation rate drops to a low value. The majority of ions are therefore formed relatively close to the rapidly-falling edge of the evaporation pulse and will experience energy losses as a result. In the case of the slow (80 or 500μS) pulses used in the present experiments, considerable specimen blunting occurred in the duration of an individual pulse, as very few ions were generally recorded on subsequent pulses. It might be argued that only a few ions would be produced on the rising edge of the pulse,

which is relatively short in duration, and the majority of the ions would be evaporated at a constant voltage during the flat top of the evaporation pulse. If this were to be correct we would expect to see a spectrum with a substantially sharper peak than in the atom-probe, which is not the case. We must therefore conclude that either (1) the width of the spectrum is due to intrinsic energy losses, which are unaffected by the evaporation pulse width, or (2) substantial numbers of ions are formed during the rising edge of the pulse, and relatively few during the peak of the pulse.

The second feature which aroused interest may be seen in fig(4.2a). In a number of the spectra obtained from molybdenum the high-energy end of the spectrum apparently contained two sharp lines; these were not seen in spectra taken from tungsten specimens which were otherwise similar to the molybdenum spectra shown. The apparent lines are largely obscured in the histograms by the large bin-width used.

The origin of these spectral lines could be due either

1) to a mere statistical fluctuation in the density of ions arriving on the detector, or

2) to a 'ripple' on the supposedly flat top of the evaporation pulse, or

3) to an intrinsic feature of the evaporation process.

Although statistical effects could in principle be eliminated by careful repetition of the experiment, it is not possible using the experimental technique described above to discriminate between the other possibilities with certainty. However, pulse effects can be eliminated by means of a simple experimental modification, which is described below. This new technique allowed the measurement of intrinsic energy losses of field-evaporated ions, for the first time.

Fig 4.4

(a)

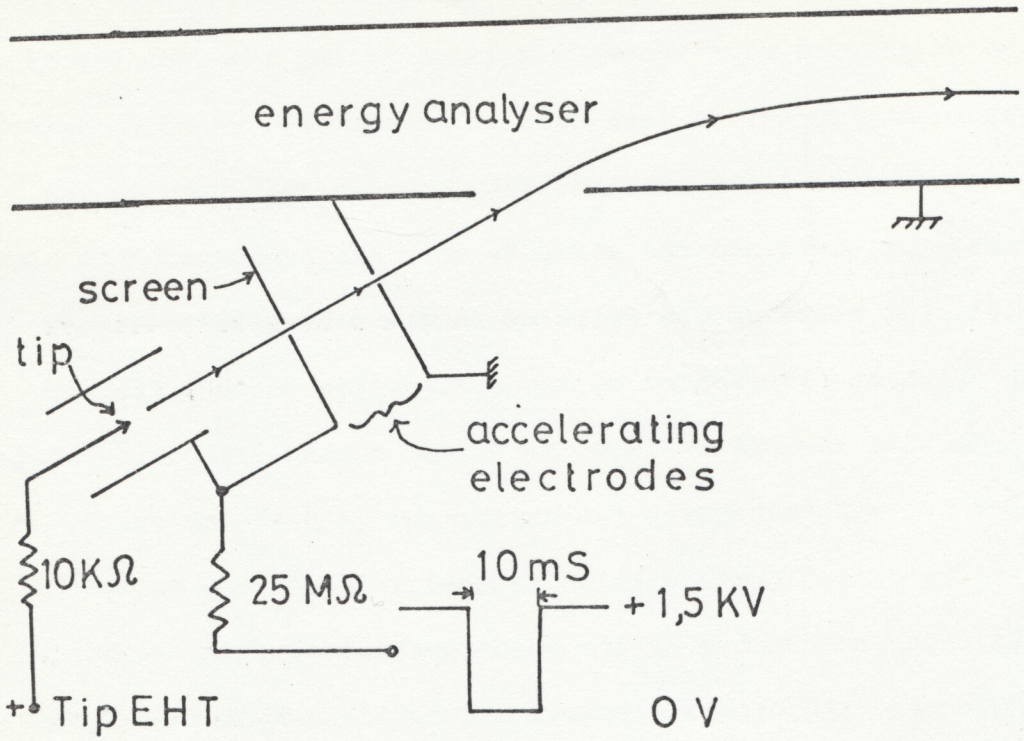
energy analyser
screen
tip
accelerating electrodes
10KΩ
25 MΩ
10 mS
+1,5 KV
+ Tip EHT
0 V

(b)

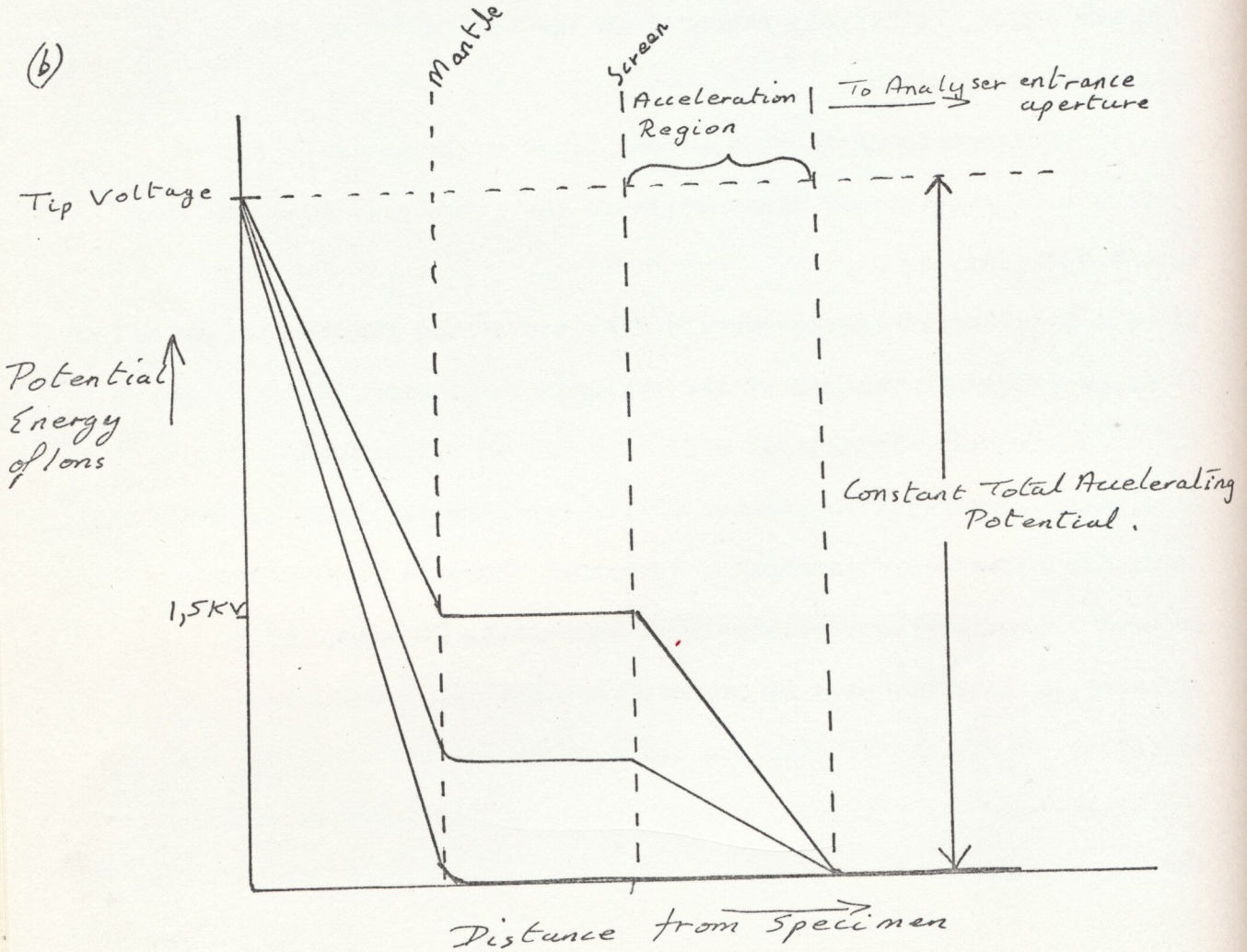
Mantle
Screen
Acceleration Region
To Analyser entrance aperture
Tip Voltage
Potential Energy of Ions
1,5KV
Constant Total Accelerating Potential.
Distance from Specimen

4.3.1 Use of an Acceleration Electrode.

The experimental technique used in these measurements is related to the technique which is used in field-ion mass-spectrometry to introduce a beam of field-ionized molecules into a magnetic spectrometer at a fixed energy (Beckey 1971). In the present experiment we wish to obtain a beam of field-evaporated metal ions which have all been accelerated through the same potential, with the energy-spread of the beam not dependent on the exact way in which the potential is applied: since the beam is to be analysed by an electrostatic spectrometer whose focussing properties depend on the angular components of the particle velocities, it is important that no unwanted lens effects are introduced in the process of obtaining the beam of ions.

An electrode assembly which meets these requirements is shown in fig(4.4). The specimen is connected to a stable voltage V by a low-value limiting resistor (10 KΩ). An electrically isolated 10 mm diameter stainless-steel mantle surrounds the specimen, and is electrically connected to the microscope phosphor screen, which is deposited on an electrically-isolated stainless-steel plate. A second, earthed, plate is positioned by alumina spacers accurately parallel to, and 10 mm behind, the phosphor screen. There is a 1,5 mm diameter probe-hole in the centre of the phosphor screen, and a 2 mm diameter hole in the second plate, to allow a selected beam of ions to pass into the spectrometer. The two probe-holes are covered by small pieces of 80% transparent 500 cpi copper micromesh, attached by conducting paint ('Aquadag') to the inside surfaces of the plates.

The electrode assembly operates in the following manner. The electric field at the specimen surface, which determines the

evaporation behaviour, is determined by the difference in potential between the specimen and the mantle/screen assembly. However, the energy of any ion which leaves the specimen and enters the spectrometer is determined by the difference in potential between the specimen and the second, earthed, electrode. In effect, the space between the screen and the second plate is an acceleration region, which accelerates the ion through the exact potential needed to give a beam of energy which is independent of the mantle voltage (fig (4.4b)). This compensation only works if the mantle voltage does not change by a significant amount during the transit time of an ion between the tip and the second electrode. For a 10 KV Ir^{2+} ion this time is approximately 300 nS. If the mantle voltage is to change by only 1 volt during this time, and a total pulse voltage of 2 KV is applied to the mantle, then the pulse risetime must be greater than 2000 x 300 nS = 600 μS. The 25 MΩ resistor in series with the pulse ensures that this condition is met, by removing any pulse component with a time-constant less than 25.10^{6} x 50.10^{-12} = 1250 μS, where 50 pF is approximately the screen stray capacity. The 10 KΩresistor in series with the specimen is sufficiently low in value to ensure that stray capacitance between the specimen and the mantle does not allow any of the 2 kV mantle pulse voltage to be coupled to the specimen; the specimen time-constant is approximately 0,5 μS and is thus too small to allow any significant proportion of the slow pulse voltage to reach the specimen. The 10 or 15 mS evaporation pulse, which is negative-going, was obtained from a vacuum-tube circuit which has been described elsewhere (Taylor 1970).

The copper micromesh in the probe-holes serves the dual purpose of preventing field penetration through the probehole and,

by defining the potential within the probehole, of ensuring that the field within the acceleration region is planar, to prevent the probehole from acting as a strong lens. The potential at the centre of a square aperture in a grid is given by (Heddle 1971, Staib 1972) $V = 16\ 10^{-2}$ Fa, where V is in volts, F is the field on one side of the aperture in volts/metre, and a is the grid repeat distance in metres. For the mesh used, the potential is approximately 1,76 volts for a field in the acceleration region of $2\ 10^5$ volts/metre. This is the worst case; since the specimen field is highest when the acceleration field is zero, most evaporated ions will pass through the grids when the field-penetration voltage is close to zero.

Strictly speaking, the acceleration region should be constructed with concentric spherical electrodes, with the specimen at the centre, so that off-axis ions are not deflected by the acceleration field. However, the half-angle of the beam selected by the probe-hole in the present apparatus is small; the exit-angle of a particle after traversing the acceleration region is given by a simple calculation as $\theta_f = \theta_o\ (1 + V/V_t)^{-\frac{1}{2}}$, where V_t is the voltage between the specimen and the screen, V is the voltage across the acceleration region, and θ_o is the entrance angle, which is small. For V_t = 10 KV, and V = 1,5 KV, $\theta_f = \theta_o$ x 0,933. The main effect of the change in angle is to cause the ions to be diverging from a source which is further from the screen; for a 10 mm acceleration region and a tip-screen separation of 40 mm , θ_{max} = 0,019 radians and the source appears to be shifted 2,8 mm from the screen, along the axis of the specimen. This shift will cause a slight worsening of the resolution of the analyser, but will not cause any shift of the focal line at the detector

(that is, no shift in the apparent energy of the beam). This was checked by monitoring the arrival position andfocus of a monoenergetic beam of helium ions, from a 10 KV specimen, as the mantle voltage was altered between + 2 KV and 0 V. No shift in the arrival position of the beam on the detector, or change in the focus, was discernible. During measurements of the energy losses of field-evaporated ions the spectrometer was aligned and focussed with the mantle set to zero, so that conditions were optimized for the metal ions.

4.3.2 Experimental Results.

As the system described above is purely electrostatic, it operates equally well for field-ionized image-gas ions or for field-evaporated metal ions, both of which will arrive at the same point on the detector if they have the same energy deficit, no matter what the mantle voltage is. This has two important consequences;

1) If the energy deficits are similar, the analyser field does not have to be altered between the setting-up process using the field-ion signal, and the evaporation process in which the image gas is pumped from the system. Any significant amount of residual gas would produce a current visible on the detector, which was not the case, even after integrating for tens of seconds; any effect of residual gases on the spectra described below is therefore believed to be negligibly small.

2) Since both the field-ion spectrum, whose energy is known from retarding-potential measurements (e.g. Tsong and Muller 1964), and the field-evaporated ion spectrum are obtained at the same specimen voltage, the absolute energy of the field-evaporated ions is available to quite high accuracy by comparison between the

Fig. 4.5

a) Tungsten-ion energy spectrum, with b) a helium-ion energy spectrum from the same specimen, for comparison.

a)

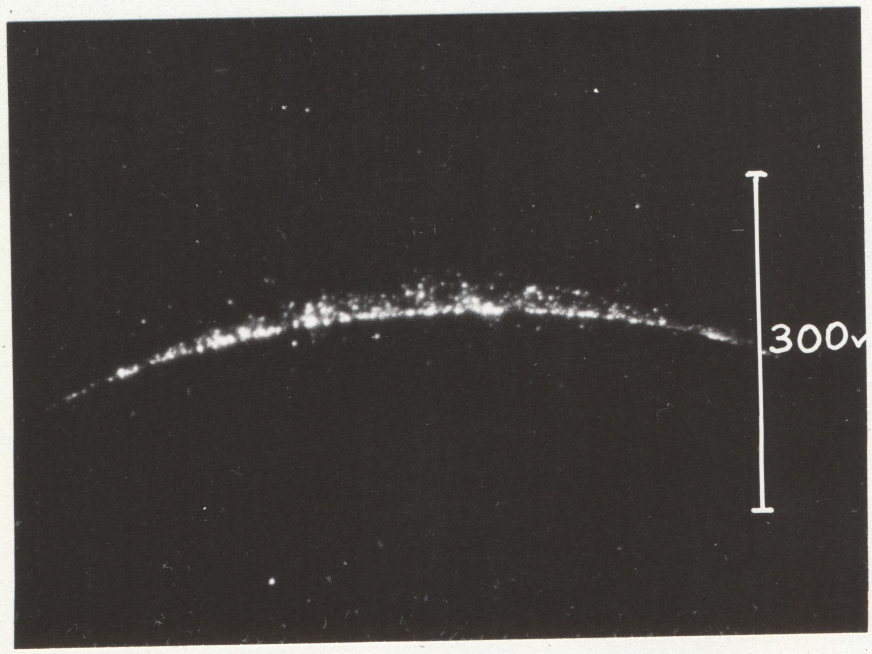

b)

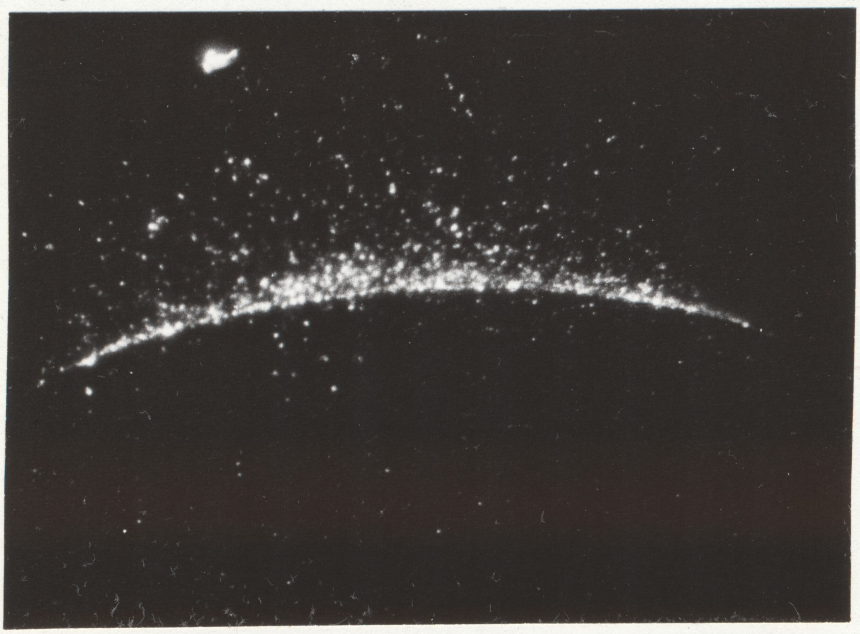

helium and metal ion spectra, and knowing the dispersion on the detector.

The spectrometer was operated in a similar manner to that originally employed for pulsed-evaporation measurements. The spectrometer was aligned and focussed on a helium field-ion signal. After checking that the analyser was properly focussed, the mantle voltage was raised to +1 KV or +1,5 KV, and the focus re-checked. The helium was then removed and the pulser used to reduce this voltage to zero for 15 mS, in synchronism with the camera flash contacts. If no evaporated ions were recorded the specimen voltage was raised and the analyser voltage reset to bring any ions back onto the detector, using a previously-prepared calibration chart. Another pulse was then applied to the mantle: if no ions were seen, the voltages were raised again; if any ions were detected, further pulses were applied until the ion flux per pulse was low again. Helium was then readmitted to the system and the position of the resulting helium-ion spectrum recorded, in order to give a calibration point for the energy-scale. The specimen voltage was then decreased by a small known amount so that the dispersion could be measured directly.

The metal-ion spectra obtained on the second or subsequent pulses of a series, or after raising the specimen voltage after previously evaporating it in vacuum, were not different in character to the first spectrum obtained. The influence of field-adsorbed contaminants may thus be discounted (as in the first pulse experiments, some tens of planes were evaporated in each pulse).

Examples of the energy spectra obtained are shown in figs (4.5), (4.6) and (4.7), and the energy deficits derived by comparison with the helium spectra are tabulated below. The following experimental results should be noted:-

1) The metal energy spectra are very narrow, with the

Fig 4.6

a) Rhodium evaporated-ion energy spectrum.

b) Helium line from the same source.

a)

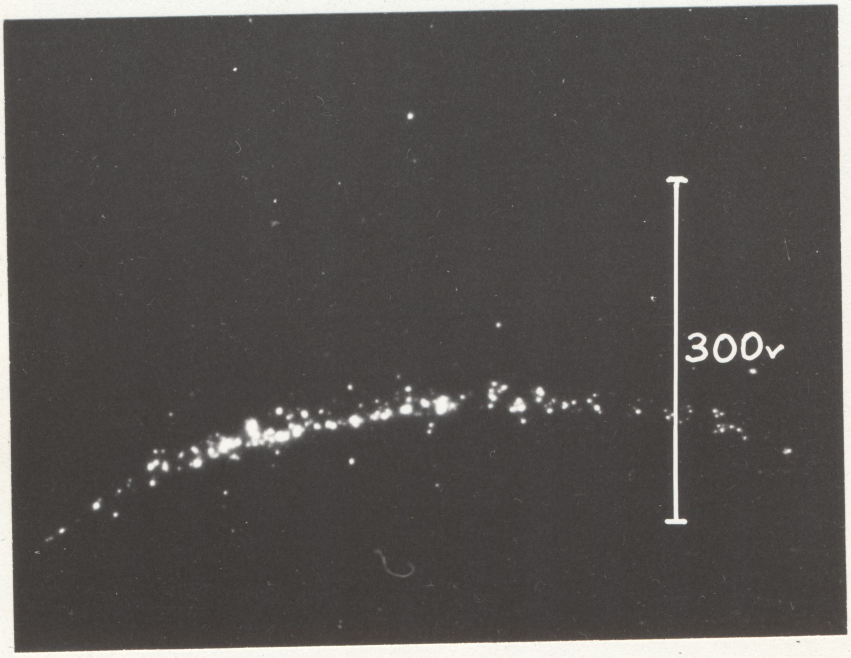

b)

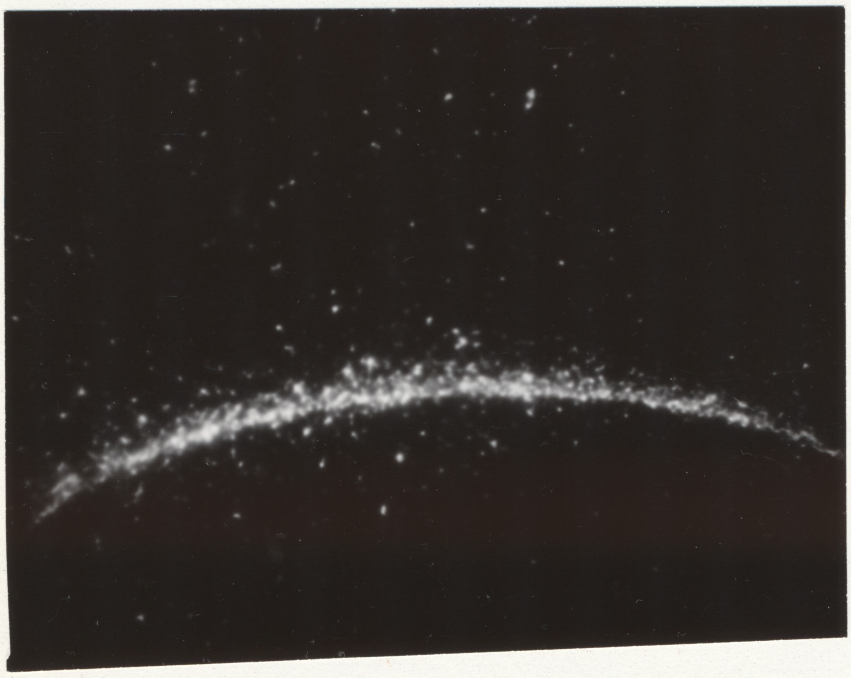

Fig. 4.7

a) Molybdenum evaporated-ion energy spectrum.

b) Helium reference spectrum.

Note the two well-resolved lines in the molybdenum spectrum.

a)

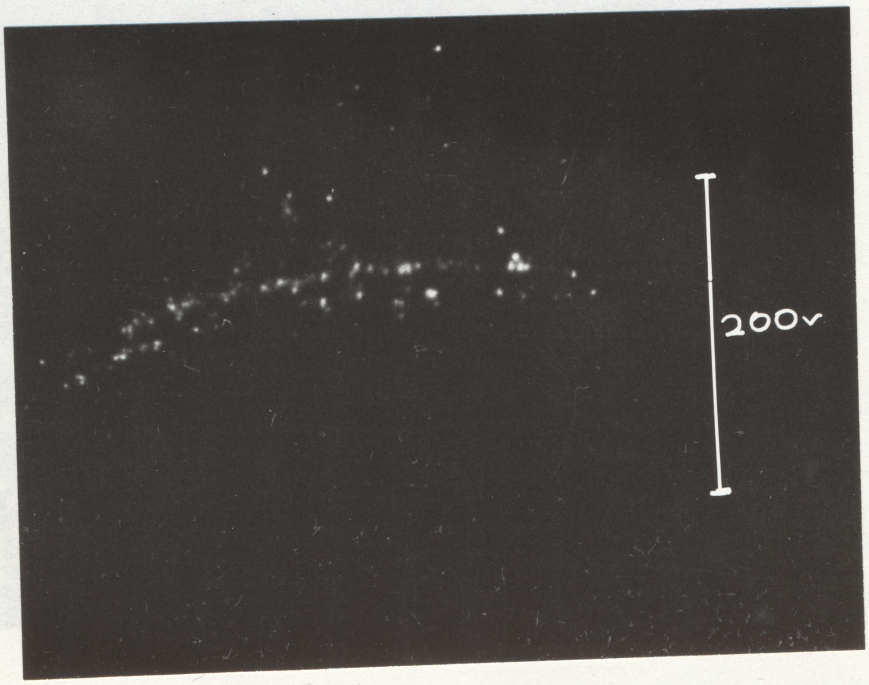

b)

great majority of the ions confined in an energy band comparable to the spectrometer resolution ($<$5 V fwhm, 20 V total); the spectra are much narrower than the original pulse-evaporation spectra ($\sim$300 V).

2) The metal ions have an energy deficit which is in the range 5 - 30 volts, depending on the metal. Molybdenum is unusual among the metals studied in showing two well-resolved spectral lines separated by some 17 V; these may perhaps be identified with Mo^{2+} and Mo^{3+} ions respectively; a magnetic spectrometer is necessary to prove this identification.

4.4 Discussion of Experimental Results.

Lucas' theory of plasmon formation (Chapter 2) should apply to the present experiment and as mentioned predicts relatively large energy losses (for W^{3+}, 252 eV, or 84 volts). This is at variance with the present results, in which the energy deficit is less than 30 volts for all the species studied so far. We may therefore conclude that the plasmon loss theory is not applicable to the formation of field-evaporated ions from relatively heavy metals, at least without some modification. Furthermore, as the energy spectra obtained in the present experiment are very narrow, it is clear that the width of the mass-peaks obtained in the atom-probe when a metal is pulse-evaporated in vacuo can be attributed to energy-deficits caused solely by pulse-effects (evaporation on the rising edge of the pulse and evaporation when the pulse voltage is about to fall).

Although the energy deficits which have been observed in these experiments are smaller than those predicted by Lucas, they are nevertheless larger than zero. No attempt has apparently

been made by other authors to predict the energy deficits to be expected from the image-force or intersection models of field-evaporation, although the energy deficit is one of the few parameters accessible to experiment. A simple treatment of the problem will be given below.

4.4.1 Theory of Energy Deficits.

If an ion is created a short distance from a metal surface, it will be attracted to the surface by the electrostatic image potential. In the presence of an electric field it will have polarization energy and can also gain energy from movement in the field. If the ion starts with zero kinetic energy at a distance x_c from the surface, it will arrive at infinity with an energy U given by

$$U = \int_{x_c}^{\infty} n\,e\,F\,dx - \tfrac{1}{2}\alpha_i F(x_c)^2 - \frac{n^2e^2}{16\pi\varepsilon_o x_c} + U_m$$

$$= neV - n\,e\,F(x_c) - \tfrac{1}{2}\alpha_i F(x_c)^2 - \frac{n^2e^2}{16\pi\varepsilon_o x_c} + U_m$$

where V is the electrical potential of the metal and U_m represents any potential energy due to interaction between the ion and the neighbouring surface atoms.

The activation energy Q_n for field-evaporation on the charge-exchange model is given by (Chapter 1)

$$Q_n = \Lambda + \sum_n I_n - n\phi - \frac{n^2e^2}{16\pi\varepsilon_o x_c} - \Delta E - \tfrac{1}{2}\Gamma - n\,e\,F\,x_c$$

$$+ \tfrac{1}{2}(\alpha_a - \alpha_i)F^2 + U_m$$

Substituting, we obtain

$$neV - U = \Lambda + \sum_n I_n - n\phi - Q_n + \tfrac{1}{2}\alpha_a F^2 - \Delta E - \tfrac{1}{2}\Gamma$$

which is the energy deficit expected on the charge exchange model. A similar deficit ($Vne - U$) is obtained from the image-force model by omitting ΔE and Γ. The actual quantity observed in the present

	eV Λ	eV ϕ	eV I_1	I_2	I_3	$(\Lambda + \sum_n I_n - n\phi)/n$ n=1	n=2	n=3	n=4	
Al	3,30	4,2	5,98	24,81	-	5,08	12,85	-	-	-
Au	3,67	4,82	9,22	20,5	-	8,07	11,88	-	-	
Be	3,45	3,92	9,32	18,21	-	8,85	11,57	-	-	
Ir	6,94	5,0	9	17	27	-	11,47	14,98	-	
Mo	6,87	4,3	7,10	16,15	27,13	-	10,76	14,78	-	
Rh	5,77	4,8	7,46	18,07	-	-	10,85	-	-	
Re	8,06	5,1	7,87	16,6	26	I_4 -	11,17	14,41	-	
W	8,80	4,5	7,98	17,7	24	35	-	15	18,9	

Experimental Values for Deficit, V.

Mo	6 ± 2 ; 23 ± 2
Re	25 ± 3
Rh	7 ± 2
W	$12,5 \pm 3$

Ionization Potentials taken from : Moore, C.E. 1958 'Atomic Energy Levels', Vol. III (N.B.S. Circular 467).

Fig. 4.8

experiment is the apparent change in specimen potential, or $(neV - U)/ne$.

Some typical values for the quantities in the equations above are tabulated in fig(4.8), and the theoretical voltage deficit calculated for the commonly-observed ionic species, assuming the energy level shift and broadening ΔE and Γ are zero; the activation energy Q_n is also taken as zero, which is close to the experimental situation ($Q_n \simeq$ leV). The effective atomic polarizability α_a is not known with any certainty; as described in Chapter 1, attempts have been made to measure α_a by using field-evaporation techniques. The deficits in the table have been calculated for $\alpha_a = 0$. The agreement between the experimental and theoretical deficits is not good; in particular, introduction of plausible values for $\frac{1}{2}\alpha F^2$ worsens the agreement for tungsten, rhodium and one of the molybdenum species. The agreement is improved by considering the energy level shift and broadening; a total value for $\frac{1}{2}\alpha F^2 - \Delta E - \frac{1}{2}\Gamma$ of about 7 eV for tungsten and rhodium is necessary for agreement. This value may not be impossibly large, as McKinstry (1972) has shown that the shift may be comparable to the coulomb potential of the ion, at the critical distance. However, the discrepancy between the observed and calculated deficit for rhenium is so large (28 eV, or 33 eV depending whether the charge of the ion is 2+ or 3+) that it seems to imply an unacceptably large value for the effective polarizability ($\sim$20 $Å^3$).

4.4.2 Multiple Charge Species and Post-Ionization.

It has been suggested by Muller that the multiple charge species observed in the atom-probe might be the result of post-ionization of field-evaporated ions. This is supported by

a one-dimensional WKB calculation by Plummer (Muller and Tsong 1973 p.99),but a one-dimensional calculation by Taylor (1970) and a 3-dimensional calculation by Chambers et al. (1971) suggest that post-ionisation is unlikely. If it were to be the cause of the appearance of multiple charge species, then the energy difference between the two species in the final spectrum may be easily calculated.

We assume that an ion of charge ne^+ becomes field-ionized to charge $(n+1)e^+$ at a critical distance corresponding to the critical distance of the normal field-ionization process: we also assume that the kinetic energy of the ne^+ ion is transferred unchanged to the $(n+1)e^+$ ion at the critical distance. Let the energy deficit of the first ion be ΔE at infinity; then, at x_c, the ion has energy $neFx_c - \Delta E$. Following post-ionization, the ion picks up further energy from the field equal to $(n+1)eV - (n+1)eFx_c$, where V is the specimen potential. The final kinetic energy of the ion is therefore

$$neFx_c - \Delta E + (n+1)eV - (n+1)eFx_c$$
$$= (n+1)eV - \Delta E - eFx_c$$
$$= (n+1)(eV - \frac{(\Delta E + I_{n+1} - \phi)}{n+1})$$

where I_{n+1} is the $(n+1)^{th}$ ionization potential of the metal.

The ne^+ and $(n+1)e^+$ ions will appear to have been accelerated by potentials differing by

$$V' = \frac{E + I_{n+1} - \phi}{n-1} - \frac{\Delta E}{n}$$
$$= \frac{n(I_{n+1} - \phi) - E}{n(n+1)}$$

For molybdenum we have, for $n = 2$, $V' = 6{,}4$ volts. Including a correction for the image potential of the Mo^{3+} ion alters this to approximately 8,5 volts. In fact, the data of fig(4.8)

show that the two lines in the energy spectrum are separated by 17 volts; the difference between experimental and theoretical results is apparently too large to be accounted for by experimental errors or theoretical approximations, and therefore does not support the post-ionization theory.

4.4.3 Post-Neutralization.

A process which is apparently as probable as post-ionization as a cause of multiple charge species is partial neutralization of a highly-charged ion by capture of an electron from the metal. A similar process has been invoked by Gomer and Swanson (1963) to account for the low yield of ions in electron-impact desorption measurements. Although this process may be expected to be relatively unlikely in field-evaporation, due to the short time-interval during which a newly-formed ion will remain sufficiently close to the surface for an electron to tunnel from one to the other, we will calculate the effect that partial neutralization would have on the energy spectrum.

The calculation follows the same lines as for post-ionization with the difference that x_c is not well defined: the electron may tunnel from any occupied level in the metal (with greater or less probability) and must find an unoccupied level in the departing ion in which to arrive.

The $(n + 1)$-charged ion arrives at x with an energy $(n + 1)eFx - \Delta E_{n+1}$, and, following partial neutralization, acquires further energy neV - neFx (ignoring image-forces for the moment). The n-charged ion has a final energy

$$ne\left(V - \frac{(\Delta E - eFx)}{n}\right)$$

The n-charged and (n+1)-charged ions will arrive at the detector with energies corresponding to a difference in acceleration potential

of $$V' = \frac{\Delta E}{n+1} - \left(\frac{\Delta E - eFx}{n} \right)$$

$$= \frac{(n+1)eFx - \Delta E}{n\,(n+1)} \quad \text{volts.}$$

For the case of molybdenum, the experimentally observed result is V' = 17 volts, and n = 2, so, substituting for the measured quantities, we obtain

$$eFx = 57 \text{ eV.}$$

For $eF = 4{,}5$ eV/A, $x = 12{,}7$ A.

This calculation suggests that if post-neutralization is to explain the observed molybdenum energy spectrum, the electron must tunnel from the metal across a distance of some 12 Angstroms into a level nearly 60 volts beneath the vacuum level of the ion. Even making allowances for experimental errors and for the (small) coulomb interaction with the metal, it seems unlikely that this is the case, unless some theoretical reason can be found for this low-lying level to be empty and especially suitable for post-neutralization.

4.5 Summary.

In the first part of this chapter the measurement of the energy spectrum of pulse-evaporated metal ions was discussed. It was found that the energy spread found using pulses of 550 μS length was similar to the energy spread found by Krishnaswamy and Muller (1973) using nanosecond-pulsed evaporation. This experiment did not show the origin of the energy-losses. However, a modification of the energy-analyser was described which allowed pulse-effects (premature evaporation, etc.) to be separated from intrinsic energy-loss processes (possible plasmon losses and losses due to the

field-evaporation process itself). The results obtained with this new technique, which are summarized below, suggest that evaporation on the rising edge of the evaporation pulse was the main cause of the energy losses in the first experiment.

Energy spectra were measured for tungsten, molybdenum, rhodium and rhenium using the modified apparatus. It was found that the spectra were narrow in width, with most ions being confined to a 5 volt range, and all ions within 20 volts of one another; comparison with helium spectra suggests that the metal spectra may well be 1 volt or less in width, or at least less than the resolution of the present analyser. The metal ions all had significant energy losses, in the range of 5-25volts (10-50 eV), deduced by comparison with the position of the helium line on the detector. Molybdenum alone produced two well-resolved spectral lines, separated by 17 volts, which were tentatively identified with the species Mo^{2+} and Mo^{3+}, which are present in roughly equal abundances in atom-probe spectra.

The energy deficits are too low to to be the result of the plasmon loss process described by the Lucas theory in its original form. The energy losses to be expected from the image-force or charge-exchange models of field-evaporation were derived; the calculated values did not compare very satisfactorily with the observed values, even allowing for the possible experimental error. Post-ionization and post-neutralization, causing the appearance of several charge-species in the evaporation products, did not fit the observed data for molybdenum.

Future work on the energy analysis of field-evaporated ions is likely to prove a fruitful source of data on field-evaporation, and will be a very useful complement to the present technique of measuring evaporation-rates as a function of field and temperature.

It is to be hoped that these techniques, used in conjunction with field-desorption microscopy, which will be described in the remainder of this dissertation, will provide enough sound experimental data to enable the present unsatisfactory state of field-evaporation theory to be remedied. Future work on energy analysis must include the development of a more accurate energy-analyser; while the analyser described above worked well up to its original specification, the data obtained with it show that an analyser with a resolution approaching 0,1 volts, or less, over a range of some 30 volts, could be usefully employed in future work.